



# Computational DFT study of the 1,3-dipolar cycloadditions of 1-phenylethyl-*trans*-2-methyl nitron to styrene and 1-phenylethyl nitron to allyl alcohol

Tapas Kumar Das, Sneha Salampuria, Manas Banerjee \*

Department of Chemistry, University of Burdwan, Burdwan 713104, India

## ARTICLE INFO

### Article history:

Received 13 April 2010

Received in revised form 4 August 2010

Accepted 4 August 2010

Available online 10 August 2010

### Keywords:

1,3-Dipolar cycloaddition

Nitrones

Transition state

Free energy of activation

Diastereomeric excess

Global electrophilicity

## ABSTRACT

Theoretical calculations were performed at the modest B3LYP/6-31G(d) level of DFT to interpret the regioselectivity and enantioselectivity and also to predict diastereofacial selectivity for 1,3-dipolar cycloaddition reaction of two known nitrones leading to a diastereomeric excess of the products. In this respect, N-substituted and C-substituted nitrones were considered for reactions with the substituted dipolarophiles like styrene and allyl alcohol. The reactions were studied by calculating the potential energy surface of the addition process and rationalizing in terms of the reactivity index of global electrophilicity. For the reactions considered, trends in reactivity, i.e., the *regio*- and *exo/endo*-selectivity and product ratios have been explained in terms of frontier orbitals interaction, electrophilicity difference, the rate constant values and an analysis of Pauling's bond order and Wiberg bond index in the transition state. All these were found to be in good agreement with the experimental findings.

© 2010 Elsevier B.V. All rights reserved.

## 1. Introduction

The chemistry of 1,3-dipoles has created great interest and application over more than a century [1]. A historical study [2] of their cycloaddition reactions has been of immense importance [3] in both academia and industry. Such reactions of the nitrones leading to 5-membered isoxazolidine rings are of particular interest in bio-organic chemistry. Considering the need for stereo-specific synthesis of the cycloadducts, theoretical prediction of the probable adducts along with their preferred reaction path would be of much importance. The mechanism of cycloaddition reactions and of those encompassing the pericyclic reactions in general, had created a lengthened debate during the 1960's and 1970's [4]. Many experimental reports and theoretical calculations continued to populate the literature over different areas of the 1,3-dipolar cycloaddition (13DC) chemistry. Keeping in mind the generally accepted views regarding these reactions [5,6], continued efforts in reconciliation between the theory and experiment are still going on [7–12]. Our interest in the present theoretical investigation stems from an attempt to provide an in-depth account of 13DC reactions of the nitrones [13]. We have taken up the present systems from literature with an aim to visualize the processes of *regio*- and *enantio*-selectivity through density functional theory (DFT) calculations. It is known that the control of stereochemistry

in the addition step leads to enantioselectivity and diastereoselectivity of the products [4]. The stereospecificity dispute had ultimately settled down in favour of the synchronous and concerted mechanism rather than the step-wise, diradical mechanism [3,14]. According to Huisgen [8], the transition state (TS) for pericyclic reactions was concerted, whereas Dewar suggested [15] it to be an asynchronous and aromatic transition state. Fukui attributed the control of 13DC to frontier molecular orbitals (FMO) of the substrates [16]. Again according to Sustmann [17,18] the classification of our reactions following Scheme 1 would be of type-I if they incorporate HOMO of the dipole to react with LUMO of 'ene' and those following Scheme 2 would be of type-II if those were effected through LUMO of dipole interacting with HOMO of 'ene'. The HOMO, LUMO energy values for all the reactants are presented in Table 1. We have displayed this observation in Fig. 1. It is well-known [4] that cycloaddition of unsaturation ('ene') to a nitron like benzonitrile oxide gives predominantly the 5-substituted isoxazolidine, a feature which is not readily explained by the polar arguments, but could be readily interpreted with mechanism involving biradical intermediates. The relative stability of the different regiomers of the biradical intermediate has been pointed out in Fig. 2. In a theoretical mechanistic study [19] of the 13DC of fulminic acid and diazomethane, the analysis was done in terms of *ab initio* MO theory instead of DFT and they have demonstrated the formation of a biradical state through cleavage of the  $\pi$ -bond of the dipolarophile.

In the present work we have considered reactions between several substituted nitrileoxides taken as the dipolar nitrones and the

\* Corresponding author. Tel.: +91 9434252709, +91 3429434252709 (Mobile); fax: +91 3422530452.

E-mail address: [manasban@rediffmail.com](mailto:manasban@rediffmail.com) (M. Banerjee).

Configuration of approaching reactants	Structure symbol, reactants	Structure symbol, products	Structure symbol, TS
si-face of nitrone + exo-ene	1sx	1psx	1tsx
si-face of nitrone + endo-ene	1sn	1psn	1tsn
re-face of nitrone + exo-ene	1rx	1prx	1trx
re-face of nitrone + endo-ene	1rn	1prn	1trn

<sup>a</sup>There are no regio- products

**Scheme 1.** Reaction of 1-phenylethyl-*trans*-2-methyl nitrone (N1) and styrene (E1)<sup>a</sup>.

Configuration of approaching reactants	Structure symbol, reactants	Structure symbol, products	Structure symbol, TS
si- face of ene + exo-nitrone	2sx	2ps	2tsx
si- face of ene + endo-nitrone	2sn	2ps	2tsn
re- face of ene + exo-nitrone	2rx	2pr	2trx
re- face of ene + endo-nitrone	2rn	2pr	2trn

<sup>b</sup>Since the nitrone C-atom is not prochiral, both exo- and endo- attacks of nitrone to si-face of allyl alcohol give the same product. Similar thing occurs for the re-face. Also there are no regio products.

**Scheme 2.** Reaction of 1-phenylethyl nitrone (N2) and allyl alcohol (E2)<sup>b</sup>.

**Table 1**

Total energy, HOMO, LUMO, chemical potential, hardness, electrophilicity of the isolated dipoles (N1 and N2), the dipolarophiles (E1 and E2) and their differences.

Global properties										
	Optimized energy (a.u.)	$\varepsilon_{\text{HOMO}}$ (eV)	$\varepsilon_{\text{LUMO}}$ (eV)	$\mu$ (eV)	$\eta$ (eV)	$\Delta\eta$ (eV)	$\omega$ (eV)	$\Delta\omega$ (eV)	$\Delta N_{\text{max}}$	$\eta^*$
N1	−518.801981	−5.543	−0.513	−3.03	5.03		0.91		0.60	
E1	−309.648272	−6.032	−0.831	−3.43	5.20	0.17	1.13	0.22	0.66	4.712
N2	−479.480661	−5.996	−0.569	−3.28	5.43		1.00		0.60	
E2	−193.108432	−6.673	0.835	−2.92	7.51	2.08	0.57	0.43	0.39	6.105

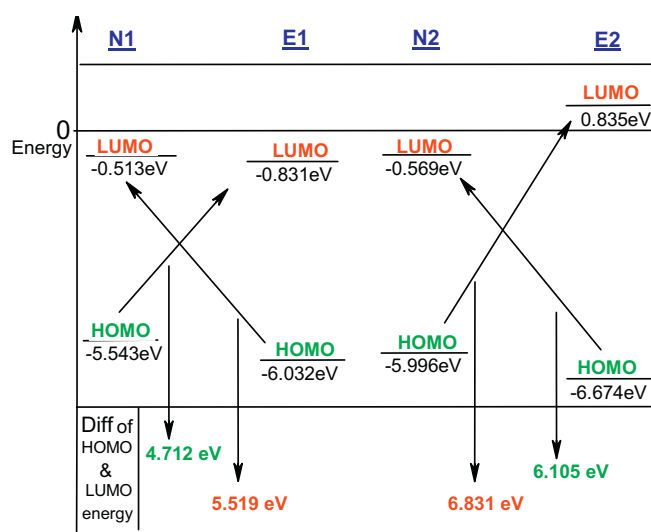


**Fig. 1.** HOMO–LUMO energy gap.

unsymmetrically substituted 'enes' like styrene and allyl alcohol. Experimental reports [20,21] about the reaction between N(1-phenylethyl)-*trans*-C-methyl nitrone (N1) and styrene (E1) shown in Fig. 3, indicate production of the exo-isomer in diastereoselective excess of the endo-isomer. A scheme for this cycloaddition reaction was very concisely presented by Belzecki and Panfil

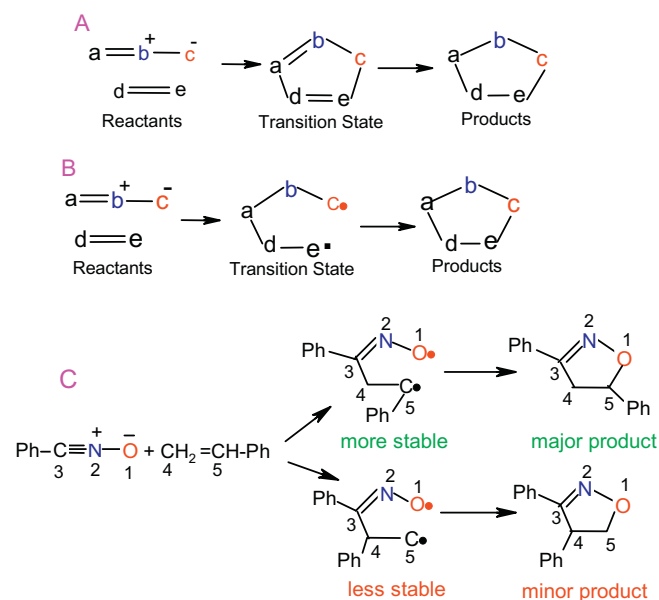


**Fig. 2.** A comparison between biradical and concerted mechanism.

[21]. We have developed calculations on the basis of their scheme and the results of our calculations are given in the subsequent sections. Very recently spiroisoxazolidines were synthesized as

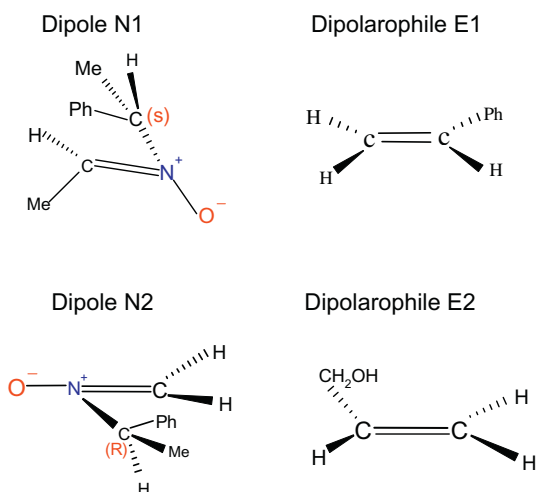


Fig. 3. The reactants N1 and E1 (Scheme 1) and the reactants N2 and E2 (Scheme 2).

antimycobacterial agents [22] from 13DC of C-aryl-N-phenyl nitrones and substituted pyridinones and were identified as potential anti-tuberculosis drug. As key steps for total synthesis of virus inhibitors, 13DC involving azides, nitrones and azomethine ylides are most appropriate [23] with high biological response. Several workers [24–28] have explored the 13DC reactions using DFT calculations along with the associated reactivity tools of hardness and softness. More recently, several workers have explored [29–31] the energetics of *stereo*- and *regio*-selectivity of 13DC reactions of nitrones using the DFT/B3LYP/6-31G(d) method. We have similarly adopted DFT/B3LYP/6-31G(d) method for calculating the energies of reactants, products and the TS. The rate constant of the addition process has been calculated by using the standard transition state theory (TST) and applied the same to rationalize the product ratios.

The control for such reactions is indeed not solely by the FMOs, but certain other parameters like hardness and electrophilicity [32–35] having definite dependence on the HOMO and LUMO have more direct influence on the reactions. Chattaraj et al. [36,37] have extensively reviewed the diverse facets of reactive and physico-chemical processes with the help of electrophilicity index defined earlier by Parr et al. [38]. Geerlings et al. [39] have reviewed the conceptual aspects of DFT and have shown how the various physicochemical parameters are derived from theory and applied successfully to chemical systems. Chemical reactivity has been correlated [40] in terms of local softness, hardness, Fukui functions and certain other response functions. Among these new concepts are the perturbative perspectives [41] on chemical reactivity. The thermodynamic analog such as electronic chemical potential, although not an observable physical quantity, has its success linked with the electron density which is instrumental in bearing most information about the ground state. It is attractive from the purview of organic chemist to examine the proximity of TS to the reactants or the products over the reaction coordinate. In this respect the Hammond postulate [42] tells that TS for exothermic reactions is more reactant-like, and for endothermic it is more product-like. We can expect that FMO effects would be particularly strong in exothermic reactions. The global electrophilicity ( $\omega$ ), chemical potential ( $\mu$ ) and hardness ( $\eta$ ) parameters help one to explore the nature of the reactions and reactivity. Theoretically calculated activation parameters for 13DC reactions, their regioselectivity and *exo/endo*-, i.e., enantioselectivity show good agreement with the experimental findings. In our previous paper, we have reported the DFT study of 13DC reaction of azomethine ylides with maleimide, maleic anhydride, methylacrylate and some simple substituted alkenes [43]. We have also explored both experimen-

tally and theoretically [44] the 13DC reaction of 1-pyrroline-1-oxide with methyl cinnamate and benzylidene acetophenone leading to different *exo/endo*-adducts due to modification of functional group in the dipolarophile moiety. In this work we have rationalized the experimentally observed products ratio. A coordination by  $Mg^{2+}$  ion in the complex formation process between benzonitrile oxides and acrylopyrazolidinone had established [45] that the complexation did not produce any change in mechanism which was asynchronous, concerted and non-polar in character, thereby presenting a 5-regioselectivity of the product.

## 2. Computational method

All our calculations were carried out on a Silicon Graphics Workstation: Octane-2 employing the UNIX version of Gaussian 03 software [46] together with Gaussview 03. Structures of the isolated reactant species and the products (adduct) were separately and individually optimized to their respective equilibrium structures through the DFT/B3LYP method, using 6-31G(d) basis set. For studying the stereochemistry of reacting systems, we have chosen this method since it gives sufficiently good results. All the reacting systems were studied by optimization of TS following the well established technique of characterizing the TS through vibrational analysis leading to a single imaginary frequency. This procedure satisfies that the potential energy curve connecting the optimized reactants and the products should pass through the TS which is a first order saddle point. This is achieved through setting the option QST 3 within the optimization step of Gaussian program, which employs a synchronous transit-guided quasi Newton (STQN) procedure [47] for locating the TS. Confirmation of the right transition structure in each case was ensured through IRC calculations on the TS which were carried out over a 31-point grid of reaction coordinate with 15 points in each of forward and reverse directions on the path. We have performed higher level single point energy calculations with the basis 6-311 + G(d,p) on the equilibrium structures previously optimized with 6-31G(d) basis [43]. In such calculations the energy differences for barriers of the reaction increased in magnitude, which are presented in Tables 2 and 3 as were also observed by others [43,48]. Activation energy for the forward reaction process was estimated by subtracting the sum of isolated reactants energies from the energy of the optimized TS. In a similar way, the free energy of activation ( $\Delta G^\ddagger$ ) were calculated from the difference of Gibb's free energies of the concerned species at 298 K. Moreover, the heats of reaction ( $\Delta_r H$ ) and free energies of reaction ( $\Delta_r G$ ) at 298 K were also calculated from the differences of the corrected enthalpies and corrected free energies, respectively of products and the reactants obtained at the B3LYP/6-31G(d) level, the values are given in Tables 4 and 5. An energy partitioning analysis [49] involving quasi-classical trajectory, containing no zero point vibrational energy was reported to reveal the synchronicity by following the dynamics of the reactants involving translational, vibrational and rotational degrees of freedom.

### 2.1. TST based reactivity parameters

To understand the nature of TS, we have calculated the index of Pauling's [50] partial bond order (PBO) which was used by Magnusson and Pranata [51] in their similar investigation. The PBO is defined as

$$\log_{10}(\text{PBO}) = -(r_{\text{TS}} - r_{\text{SB}})/0.71 \quad (1)$$

where  $r_{\text{SB}}$  is the length of a single bond between two atoms, as observed in the product, and  $r_{\text{TS}}$  is the length of the same bond in the TS, involving only the representative non-metallic 1st row elements.

**Table 2**Energy data for the reaction: 1-phenylethyl-*trans*-2-methyl nitron (N1) with styrene (E1), giving normal product isomer.<sup>a</sup>

Orientation complex optimized (Energy in a.u.)		Products optimized (Energy in a.u.)		Transition states (Energy in a.u.)		
				$E_{act}$ (kcal/mol) [6-31G(d)]		$E_{act}$ (kcal/mol) [6-311 + G(d,p)]
1sx	–828.454835	1psx	–828.478962	–828.420823	18.47	22.39
1sn	–828.455172	1psn	–828.482870	–828.418012	20.23	24.88
1rx	–828.456308	1prx	–828.485254	–828.425407	15.59	19.09
1rn	–828.457253	1prn	–828.475033	–828.423839	16.58	21.04

<sup>a</sup> There was no regio-product, computationally.**Table 3**Energy data for the reaction: 1-phenylethyl nitron (N2) with allyl alcohol (E2), giving normal product isomer.<sup>b</sup>

Orientation complex optimized (Energy in a.u.)		Products optimized (Energy in a.u.)		Transition states (Energy in a.u.)		
				$E_{act}$ (kcal/mol) [6-31G(d)]		$E_{act}$ (kcal/mol) [6-311+G(d,p)]
2sx	–672.594015	2ps	–672.636686	–672.570344	11.77	15.76
2sn	–672.598137	2ps	–672.636684	–672.570974	11.37	16.67
2rx	–672.596509	2pr	–672.639134	–672.571198	11.23	15.72
2rn	–672.596769	2pr	–672.639134	–672.564967	15.14	21.15

<sup>b</sup> There was no regio-product, computationally.**Table 4**Free energy of activation, enthalpy of activation, rate const. and enthalpy of reaction: 1-phenylethyl-*trans*-2-methyl nitron (N1) with styrene (E1).

Reaction considered	Free energy of activation $\Delta G^\ddagger$ (in kcal/mol)	Enthalpy of activation $\Delta H^\ddagger$ (in kcal/mol)	Numerical values of the rate constant $k_1$	Enthalpy of reaction $\Delta_r H$ (in kcal/mol)
1sx to 1psx	33.37	19.30	$1.7 \times 10^{-12}$	–15.14
1sn to 1psn	36.14	21.01	$1.6 \times 10^{-14}$	–23.79
1rx to 1prx	30.51	16.21	$2.2 \times 10^{-10}$	–19.10
1rn to 1prn	31.51	17.22	$4.1 \times 10^{-11}$	–12.63
Average, $k_1 = 6.6 \times 10^{-11}$				

**Table 5**

Free energy of activation, enthalpy of activation, rate const. and enthalpy of reaction: 1-phenylethyl nitron (N2) with allyl alcohol (E2).

Reaction studied	Free energy of activation $\Delta G^\ddagger$ (in kcal/mol)	Enthalpy of activation $\Delta H^\ddagger$ (in kcal/mol)	Numerical values of the rate constant $k_2$	Enthalpy of reaction $\Delta_r H$ (in kcal/mol)
2sx to 2ps	26.39	12.75	$2.4 \times 10^{-7}$	–26.51
2sn to 2ps	26.29	12.48	$2.8 \times 10^{-7}$	–26.74
2rx to 2pr	25.36	12.22	$1.4 \times 10^{-6}$	–27.99
2rn to 2pr	31.06	16.38	$8.8 \times 10^{-11}$	–27.99
Average, $k_2 = 4.8 \times 10^{-7}$				

The rate constant value for the bimolecular addition reaction can be simply estimated with the help of transition state theory. The Eyring equation for the rate constant in TST can be written as [52],

$$k = \frac{k_B T}{h c^\circ} e^{-\frac{\Delta G^\ddagger}{RT}} \quad (2)$$

where  $k_B$  is Boltzmann constant,  $h$  is the Planck constant,  $c^\circ$  is the standard-state concentration (often taken to be  $1.00 \text{ mol dm}^{-3}$ ) and  $R$  is gas constant [52]. From this Eq. (2) we calculated the rate constants for different paths of the reaction, i.e., different reactive channels (*exo/endo*-) on different faces and the same are presented in Tables 4 and 5. This helps us to predict the probable products ratio.

## 2.2. DFT based reactivity parameters

While the conceptual DFT approach to chemical reactivity [39] has been outlined, for the simple purpose of quantification in our reacting systems the following computational scheme was adopted.

With the help of density based descriptors, the reactivity can be explained by a very simple operational formulation in terms of the one-electron FMO energies, viz. the HOMO and LUMO energies, given by [53]  $\mu$  the chemical potential,

$$\mu \approx (\epsilon_{\text{HOMO}} + \epsilon_{\text{LUMO}})/2.$$

However, the chemical hardness specifies the resistance to this electronic change occurring during the cycloaddition [54] and can be quantitatively represented by

$$\eta \approx \epsilon_{\text{LUMO}} - \epsilon_{\text{HOMO}}$$

The global electrophilicity index [38]  $\omega$  measures the stabilization in energy when the system acquires an additional electronic charge  $\Delta N$  from the environment. It can be simply expressed in terms of electronic chemical potential and hardness as

$$\omega = \mu^2/2\eta$$

The maximum amount of electronic charge  $\Delta N_{\text{max}}$  that can be accepted by an electrophile system is given by [38]

$$\Delta N_{\text{max}} = -\mu/\eta$$

The global electrophilicity index includes the propensity of the electrophile to acquire an additional electronic charge as well as the resistance to exchange the electronic charge with the environment simultaneously. Thus, a good electrophile can be characterized by a high value of  $\mu$  and a low value of  $\eta$  [36,37].

### 3. Results and discussion

The results obtained from our theoretical calculations are divided into three sections and presented hereunder.

#### 3.1. Reaction of the nitrones with styrene

In this section we present our results for reaction between the N-phenylethyl substituted nitrone (N1) and dipolarophile (E1) the structures being shown in Fig. 3 and the experimental reports [20,21] for which were available. Belzecki et al. had studied the reaction of N1 and E1. We had pictorially represented their approach for reaction through different reactive channels on the different faces in Fig. 4. We had investigated computationally the different reactive channels (*exo*- and *endo*-) of styrene adding towards the *re*- and *si*-faces of nitrone as labeled in Scheme 1. Structure symbols for the various products (*psx*, *prx*, *psn*, *prn*) together with their corresponding TS (*tsx*, *trx*, *tsn*, *trn*) are defined in Scheme 1 in order to label the various stereochemical species. For the approaching orientation of reactants, the structural naming convention [43]: [(*re*/*si*)(*exo*/*endo*)] and for the product/transition state species the structural naming convention: [(*product*/*ts*)(*re*/*si*)(*exo*/*endo*)] have been followed. Those naming are concisely presented in the following schemes.

As each product in present system contains two chiral centers in the isoxazolidene moiety, one coming from the dipole and one from the dipolarophile, there should exist four stereo-isomers among the products. In Table 2 it is found that for reaction of N1 and E1, the *exo*-path involves lesser activation energy than the *endo*- path in both *re*- and *si*-faces giving the normal isomer (substituent entering 5-position of the ring). The *exo*-products *prx* and *psx* are thus expected to be generated in excess as the major kinetic products over *prn* and *psn*, agreeing well with experimental outcome. For adding further precision to our results we have performed higher level single point energy calculations with the basis 6-311 + G(d,p) on the equilibrium structures previously optimized with 6-31G(d) basis, and obtained moderate barrier heights ( $\Delta E^\ddagger$ ) which are shown in Table 2. This type of results were also obtained in our previous paper [43]. The computed results so obtained are more appropriate to explain the experimental results and can

quantify the barriers reasonably. The electron withdrawing phenyl group in the substituent of the dipolarophile could be the cause for favouring the *exo*-attack. Again any attempt to generate the corresponding regiomers from N1 and E1 had failed because all the starting opposite orientations of the reactants had led finally to unrealistic and totally different structures having no relevance with the optimized product. This consequence has been supported by the experimental existence of only two stereoisomers, among which prominence of *exo*-product is consistent with its lower activation energy as shown in Table 2. Again, for obtaining further improvement of results we have calculated the ZPE corrected Gibb's free energy and enthalpy of the reactants and TS in each case and have correspondingly calculated the free energy of activation  $\Delta G^\ddagger$ , enthalpy of activation  $\Delta H^\ddagger$  and the heat of reaction  $\Delta_r H$  at 298 K. These values are presented in Table 4. Similar results [7–13,20,21,51] arrived by earlier investigators both theoretically and experimentally had led to conclusion that the substituents enter preferentially at the 5-position of the isoxazolidines.

Now from the data in Table 6, we find that in TS the newly forming C–C bond distances are smaller ( $\sim 2.0$  Å) than the C–O bond distances ( $\sim 2.35$  Å). Moreover, the PBO values in the various TS for different reactive channels are around 0.05 for C–O bonds and around 0.16 for C–C bonds which indicate the TS to be asynchronous. Calculation of local electrophilicity using the Mulliken population analysis sometimes fail to predict the preferred regioselectivity. Other types of population analysis scheme, such as electrostatic potential driven charge, Natural Bond order (NBO), etc. could be explored in this matter. From the calculation of NBO based Wiberg bond indexes we have reported the bond order values in the TS in different reactive channels. The newly forming C–O bond order found to be 0.256 is clearly less than that of the newly forming C–C bond order 0.446. This feature also confirms that the TS were asynchronous.

From the values of rate constant in Table 4 as obtained from Eq. (2), we calculated the products ratio which could be conveniently expressed according to the following expressions:

$$k_{\text{exo}/\text{si}} + k_{\text{exo}/\text{re}} = k_{\text{exo}/\text{total}} = 2.2 \times 10^{-10} \text{ and } k_{\text{endo}/\text{si}} + k_{\text{endo}/\text{re}} = k_{\text{endo}/\text{total}} = 4.1 \times 10^{-11}$$

The *exo* to *endo* ratio of overall product formation is thus

$$k_{\text{exo}/\text{total}}/k_{\text{endo}/\text{total}} = 2.2 \times 10^{-10}/4.1 \times 10^{-11} = 5.48.$$

This result is in excellent agreement with the experimental results (*exo* to *endo*-isomers was obtained in the ratio between 68:32 and 87:13), reported by Belzecki and Panfil [20].

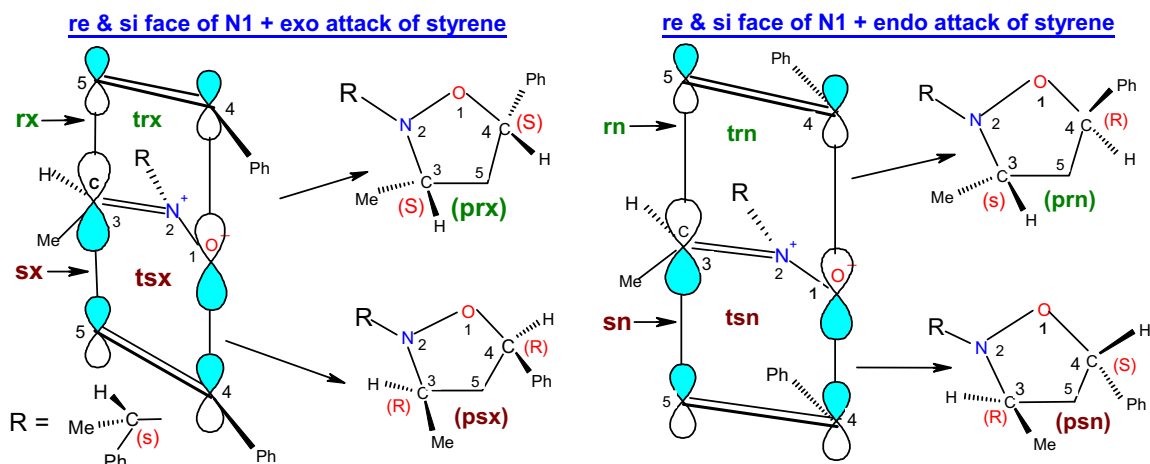
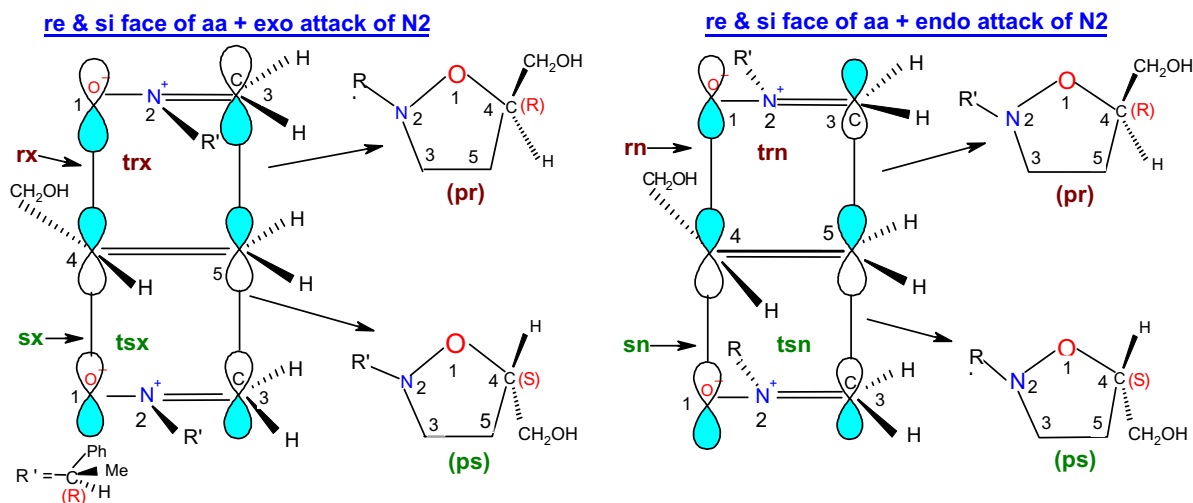


Fig. 4. The transition states and products in different (*re*- and *si*-) facial attacks to the substituted nitrone N1 (at the middle) by styrene E1 in *exo*- and *endo*-approaches.



**Table 6**Bond orders and bond distances in transition states of the reaction: 1-phenylethyl-*trans*-2-methyl nitron (N1) with styrene (E1).

Name of the TS	Pauling's bond order analysis				Wiberg bond index	
	$r_{C-O}$	$r_{C-C}$	$(PBO)_{C-O}$	$(PBO)_{C-C}$	$(NBO)_{C-O}$	$(NBO)_{C-C}$
1tsx	2.37	2.05	0.046	0.192	0.2604	0.4578
1tsn	2.38	2.03	0.047	0.100	0.2542	0.4807
1trx	2.36	2.10	0.051	0.172	0.2513	0.4229
1trn	2.32	2.11	0.056	0.158	0.2594	0.4222

**Fig. 5.** The transition states and products in different (*re*- and *si*-) facial attacks to the allyl alcohol E2 (at the middle) by substituted nitron N2 in *exo*- and *endo*-approaches.

Quantitative characterization of reactivity in DA and 13DC reactions in terms of global electrophilicity power was developed and applied [32,35] by Domingo et al. In their review Chattaraj et al. [36,37] have reported that “Larger electrophilicity differences correspond to faster reactions”. In our present study we observed similar trends: the  $\Delta\omega$  for reaction Scheme 1 is 0.22 (eV) and that for the reaction Scheme 2 is 0.43 (eV), given in Table 1. The average rate constant values could be found in Tables 4 and 5 indicating fair agreement with experiment. The greater electrophilicity difference (0.43 eV) for the pair of reactants N2 and E2 than that for the N1 and E1 pair (0.22 eV) provides the source of higher driving strength ( $k_2$ ) for the former reaction. It was found experimentally that the cycloaddition reaction between N1 and E1 produced poorer yields due to slower reaction rate. Thus, it might be concluded that the reactivity predicted in terms of global electrophilicity index showed good agreement with the experimental findings.

The structures of reacting systems N1, E1 and N2, E2 are shown in Fig. 3. In Table 1 we have presented the HOMO and LUMO energies of all the reactants along with their electronic chemical potential ( $\mu$ ), chemical hardness ( $\eta$ ) and the global electrophilicity ( $\omega$ ). According to the absolute scale of electrophilicity [37] based on the  $\omega$  index, E1 can be classified as a strong electrophile whereas the dipole N1 belongs to the realm of moderate electrophile for the reaction Scheme 1. But in the reaction Scheme 2, nitron N2 can be classified as a strong electrophile whereas the dipolarophile E2 belongs to moderate electrophile. The electronic chemical potential value of N1 (−3.03 eV) is higher than that of E1 (−3.43 eV) implying that the CT will take place from the dipole to the dipolarophile in this cycloaddition resulting in a normal electron demand (NED) reaction [32]. Since the electronic chemical potential value of E2 (−2.92 eV) is higher than that of N2 (−3.28 eV) presented in Table 1, this will imply that the CT will take place from the dipolarophile to the dipole in this cycloaddition also resulting

in a NED reaction. The pair hardness [55,56] parameter  $\eta^*$  for the pair of reactants N1 and E1 in Scheme 1 is lesser than that for N2, E2 pair in Scheme 2 provided in Table 1, reflecting enhanced exothermicity in the latter reaction which is also in agreement with the calculated values of  $\Delta_r H$  presented in Tables 4 and 5. This fact further substantiates the reliability of our DFT based results.

### 3.2. Reaction of nitrones with allyl alcohol

Tice and Ganem [57] carried out the reaction of N2 and E2. We have pictorially presented their scheme of reaction through different reactive channels on different faces in Fig. 5. The dipolarophile containing the relatively less electron withdrawing group –  $\text{CH}_2\text{OH}$  than the phenyl group has been investigated computationally in our present study. Structural naming systems similar to those given in Scheme 1 are used for the reaction between N2 and E2, in the Scheme 2.

In connection with regioselectivity of 13DC reactions, Magnuson and Pranata [51] made the general conclusion that for dipolarophiles having electron donating groups, the favoured orientation would be that of the normal adduct isomer having the substituent at 5-position of the ring, whereas for dipolarophiles having electron withdrawing groups, it would be the regioisomer with substituent at the 4-position. It has been reported [3] experimentally that the phenyl group in styrene goes to 5-position of the ring leading to the normal isomers and we have also found the same thing to occur in our TS optimization calculations. With regard to Magnuson's observation, the phenyl group is considered as having  $\pi$ -donating effect as well as  $-\text{R}$  effect of attracting electron density, the former dominating in overall, the phenyl could be considered as normal orienting in this reaction. For allyl alcohol, the primary alcoholic group  $-\text{CH}_2\text{OH}$  being less withdrawing than phenyl has been found in our calculations to be normal orienting

**Table 7**

Bond orders and bond distances in transition states of the reaction: 1-phenylethyl nitron (N2) with allyl alcohol (E2).

Name of the TS	Pauling's bond order analysis				Wiberg bond index	
	$r_{C-O}$	$r_{C-C}$	$(PBO)_{C-O}$	$(PBO)_{C-C}$	$(NBO)_{C-O}$	$(NBO)_{C-C}$
2tsx	2.26	2.09	0.071	0.168	0.2929	0.4275
2tsn	2.20	2.15	0.089	0.137	0.3093	0.4005
2trx	2.23	2.13	0.075	0.146	0.2955	0.4023
2trn	2.17	2.08	0.093	0.172	0.3365	0.4493

and depicted in Fig. 5 which is in compliance with experimental findings.

In Fig. 5 the different attacks by N2 to the two faces of E2 possessing one prochiral centre have been shown. It follows from molecular symmetry as evident from Fig. 5 that *exo*- and *endo*-attacks on either of the *re*- or *si*-faces of the alcohol lead to the same product on each face. Experimentally, the two products *ps* and *pr* were obtained in 1:1 ratio. From the values of  $E_{act}$  in Table 3, we predict that while in the *re*-face the *exo*-attack is favoured the difference in activation barriers between *exo*- and *endo*-channels in the *si*-face is too small for an enantioselectivity. The difference however increased a little by using 6-311 + G(d,p) basis set of calculation and has indicated a favourable *exo*-selectivity. Other things remaining identical we may assume that their frequency factors are almost equal and the ratio of their diastereomeric products (*ps*:*pr*) should be very close to 1:1, as may be found from their comparable values of  $\Delta G^\ddagger$  in Table 5. The product ratio obtained experimentally can be explained theoretically with our computational results as given below:

$$k_{ps} = k_{ps(si/exo)} + k_{ps(si/endo)} = 5.2 \times 10^{-7} \approx 10^{-6} \text{ and } k_{pr} \\ = k_{pr(re/exo)} + k_{pr(re/endo)} = 1.3 \times 10^{-6} \approx 10^{-6}$$

Therefore, the ratio of the formation of diastereomeric products (*ps*:*pr*) is  $k_{ps}/k_{pr} = 1$ . This value is in good agreement with the experimental results reported by Tice and Ganem [57].

About quantification of reactivity in terms of global electrophilicity for DA and 13DC reactions it has been remarked [36] that “the larger electrophilicity differences correspond to faster reactions”. As the hardness difference in Table 1 for N2–E2 system is higher, it may be noted that the reaction is accompanied with a decrease in activation energy as compared to that in the N1–E1 reaction, given in Tables 2 and 3. This feature is a consequence of the “Hardness maximization principle” [56]. It should be highlighted additionally that the HOMO–LUMO gap, even for different species, is a measure of stability in terms of the maximum hardness principle. Hard interactions are essentially electrostatic in nature. Charges or the appropriately associated quantities like molecular electrostatic potentials and local hardness are supposed to be better descriptors for hard–hard reactions. From this outlook one can get a qualitative perspective for the enhanced reactivity of the N2–E2 system.

Now from the Table 7, we found that in TS the newly forming C–C bond distances are smaller ( $\sim 2.0$  Å) than the C–O distances ( $\sim 2.2$  Å). Moreover the PBO values in the TS in different reactive channels are around 0.08 for C–O bonds and around 0.16 for C–C bonds which indicates that the TS is asynchronous. From a similar analysis of NBO based Wiberg bond indexes given in Table 7, it is also indicated that the TS is asynchronous.

### 3.3. Nature of transition state in the reactions

While the cycloaddition reactions pass through a transition state there remains to answer the question as to whether the reactions considered follow a concerted or a diradical path. Although the

accepted opinion in this regard was in favour of the concerted mechanism, at a certain stage Huisgen [14,58] reported the well-documented example of a step-wise 13DC involving an intermediate which encouraged Firestones's contention [59] that ‘no degree of stereospecificity could rule out diradical mechanism’, gaining support from his initial proposal [4] that activation energy for single bond rotation was greater than that for either formation of the second bond leading to the adduct or reversion to the reactants. In this connection we have calculated the PBOs and NBOs for C–C and C–O bonds in the TS presented in Tables 6 and 7. It can be seen from Table 7 that in TS for the reaction of E2 and N2 the C–C bond is formed early with a shorter  $r_{C-C}$  distance than the  $r_{C-O}$ , the bond order values agreeing correspondingly with bond distances. The reaction in this case can be sufficiently considered to be asynchronous and concerted. A similar theoretical investigation of mechanism and regioselectivity for 13DC of diazomethane with methylacrylate has concluded [60] the process to be asynchronous and concerted. The work has also rationalized regioselectivity by FMO model and density derived philicity indexes.

In the case of nitron N1 reacting with E1 the stereo-specific (*exo/endo*) magnitudes of activation energies are given in Table 2 and the trend of PBO values in Table 6 which are similar to those for the reaction of N2 and E2 in Tables 3 and 7. This comparative feature became prominent only after improving the results with higher level single point calculations without which the barrier energy differences were too small (less than 1 kcal/mol) to make a conclusion. Even if the possibility of a diradical mechanism is ruled out, it may be concluded that the process is highly asynchronous which was predicted at some stage by Dewar [15]. In our present work we reported only about our observations. On ground of the results of calculation in terms of FMO's interaction depicted in Fig. 1, the system N1–E1 being controlled by  $HOMO_{dipole}-LUMO_{alkene}$  interaction will be denoted as type-I under Scheme 1, whereas the reacting system N2–E2 controlled by  $LUMO_{dipole}-HOMO_{alkene}$  be denoted as type-II under the Scheme 2 [61]. An analysis of amplitudes of the reacting atoms within the corresponding interacting FMOs can provide a further rationale behind the preferred regioselectivity of the reaction. It must be understood that the control for such reactions does not lie solely with the FMOs, but depends strongly on certain other parameters like hardness and electrophilicity [25,26,29,30] possessing definite dependence on the HOMO and LUMO and bearing direct influence on the course of the reaction.

## 4. Conclusions

The 1,3-dipolar cycloaddition reactions of two well-known nitrones with two selected alkenes have been studied in detail using the B3LYP/6-31G(d) method. The experimentally found products, and the relative proportion of yields of different product isomers have been rationalized using theoretically calculated potential energy barriers, rate constants and reactivity parameters. This type of investigation can be easily extended to larger natural systems of stereochemical significance in asymmetric synthesis.

## Acknowledgement

One author, Mr. T.K. Das is grateful to the Department of Chemistry, Burdwan University for extending computational support.

## Appendix A. Supplementary data

Results of IRC calculations for the transition states together with input geometries for the systems and also the standard orientation coordinates and thermo-chemical data for the optimized structures of the individual reactants and TS together with the Wiberg bond index matrices are provided as supplementary data file 'supmt-data' which can be availed from website of the journal/publisher or from the author.

Supplementary data associated with this article can be found, in the online version, at doi:10.1016/j.theochem.2010.08.001.

## References

- [1] T. Curtius, Ber. Dtsch. Chem. Ges. 16 (1883) 2230.
- [2] R. Huisgen, in: A. Padwa (Ed.), 1,3-Dipolar Cycloaddition Chemistry, Wiley, New York, 1984.
- [3] K.V. Gothlf, K.A. Jorgensen, Chem. Rev. 98 (1998) 863.
- [4] K.N. Houk, J. Gonzalez, Y. Li, Acc. Chem. Res. 28 (1995) 81.
- [5] P. Merino, T. Tejero, U. Chiacchio, G. Romeo, A. Rescifina, Tetrahedron 63 (2007) 1448.
- [6] L.R. Domingo, M.J. Aurell, M. Arnó, J.A. Sáez, J. Mol. Struct.: THEOCHEM 852 (2008) 46.
- [7] M.T. Nguyen, A.K. Chandra, S. Sakai, K. Morokuma, J. Org. Chem. 64 (1999) 65.
- [8] M.A. Silva, J.M. Goodman, Tetrahedron 56 (2002) 3667.
- [9] C. Di Valentin, M. Freccero, R. Gandolfi, A. Rastelli, J. Org. Chem. 65 (2000) 6112.
- [10] M. Carda, R. Portoles, J. Murga, H. Roper, J. Org. Chem. 65 (2000) 700.
- [11] J. Liu, S. Niwayama, Y. You, K.N. Houk, J. Org. Chem. 63 (1998) 1064.
- [12] F.P. Cossio, I. Morao, H. Jiao, P.V.R. Scheleyer, J. Am. Chem. Soc. 121 (1999) 6737.
- [13] A. Banerji, P. Sengupta, J. Indian Inst. Sci. 81 (2001) 313.
- [14] R. Huisgen, J. Org. Chem. 33 (1968) 2291.
- [15] M.J.S. Dewar, J. Am. Chem. Soc. 106 (1984) 209.
- [16] K. Fukui, Acc. Chem. Res. 4 (1971) 57.
- [17] R. Sustmann, Tetrahedron Lett. (1971) 2717.
- [18] R. Sustmann, Pure Appl. Chem. 40 (1974) 569.
- [19] S. Sakai, M.T. Nguyen, J. Phys. Chem. A 108 (2004) 9169.
- [20] C. Belzecki, I. Panfil, J. Chem. Soc. Chem. Commun. (1977) 303.
- [21] C. Belzecki, I. Panfil, J. Org. Chem. 44 (1979) 1212.
- [22] R.S. Kumar, S. Perumal, K.A. Shetty, P. Yogeeswari, D. Sriram, Eur. J. Med. Chem. 45 (2010) 124.
- [23] C. Najera, J.M. Sansano, J. Org. Biomol. Chem. 7 (2009) 4567.
- [24] A.K. Chandra, M.T. Nguyen, J. Phys. Chem. A 102 (1998) 6181.
- [25] T.N. Le, L.T. Nguyen, A.K. Chandra, F.D. Proft, P. Geerlings, M.T. Nguyen, J. Chem. Soc. Perkin Trans. 2 (2) (1999) 1249.
- [26] L.T. Nguyen, F.D. Proft, A.K. Chandra, T. Uchimaru, M.T. Nguyen, P. Geerlings, J. Org. Chem. 66 (2001) 6096.
- [27] A.K. Chandra, M.T. Nguyen, J. Comput. Chem. 19 (1998) 195.
- [28] J. Korchowiec, A.K. Chandra, T. Uchimaru, J. Mol. Struct. THEOCHEM 572 (2001) 193.
- [29] L.R. Domingo, Eur. J. Org. Chem. (2000) 2273.
- [30] M.L. Kuznetsov, L.V. Kozlova, A.I. Dementev, Russian J. Inorg. Chem. 51 (2006) 1602.
- [31] P. Merino, J. Revuelta, T. Tejero, U. Chiacchio, A. Rescifina, G. Romeo, Tetrahedron 59 (2003) 3581.
- [32] P. Pérez, L.R. Domingo, M.J. Aurell, R. Contreras, Tetrahedron 59 (2003) 3117.
- [33] P. Pérez, L.R. Domingo, A. Aziman, R. Contreras, in: A. Toro-Labbe (Ed.), Theoretical Aspects of Chemical Reactivity, Elsevier Science, New York, 2007.
- [34] L.R. Domingo, E. Chamorro, P. Perez, J. Phys. Chem. A 112 (2008) 4946.
- [35] L.R. Domingo, M.J. Aurell, P. Pérez, R. Contreras, Tetrahedron 58 (2002) 4417.
- [36] P.K. Chattaraj, D.R. Roy, Chem. Rev. 107 (2007) 46.
- [37] P.K. Chattaraj, U. Sarkar, D.R. Roy, Chem. Rev. 106 (2006) 2065.
- [38] R.G. Parr, L.V. Szentpaly, S. Liu, J. Am. Chem. Soc. 121 (1999) 1922.
- [39] P. Geerlings, F.De. Proft, W. Langenaeker, Chem. Rev. 103 (2003) 1793.
- [40] H. Chermette, J. Comput. Chem. 20 (1999) 129.
- [41] P.W. Ayers, J.S.M. Anderson, L.J. Bartolotti, Int. J. Quantum Chem. 101 (2005) 520.
- [42] G.S. Hammond, J. Am. Chem. Soc. 77 (1955) 334.
- [43] T.K. Das, M. Banerjee, J. Phys. Org. Chem. 23 (2009) 148, doi:10.1002/poc.1597.
- [44] N. Acharjee, T.K. Das, M. Banerjee, A. Banerji, T. Prangé, J. Phys. Org. Chem. (2010), doi:10.1002/POC.1690.
- [45] L.R. Domingo, M.J. Aurell, R. Jalal, M. Esseffar, J. Mol. Struct.: THEOCHEM 942 (2010) 26.
- [46] M.J. Frisch et al., Gaussian 03, Revision D. 01, Gaussian Inc., Wallingford, CT, 2004.
- [47] C. Peng, P.Y. Ayala, H.B. Schlegel, M.J. Frisch, J. Comput. Chem. 17 (1996) 49.
- [48] L.R. Domingo, J. Org. Chem. 64 (1999) 3922.
- [49] L. Xu, C.E. Doubleday, K.N. Houk, J. Am. Chem. Soc. 132 (2010) 3029.
- [50] L. Pauling, The Nature of Chemical Bond, third ed., Cornell University, Ithaca, NY, 1960.
- [51] E.C. Magnuson, J. Pranata, J. Comput. Chem. 19 (1998) 1795.
- [52] D.A. McQuarrie, J.D. Simon, Physical Chemistry, Viva Books Private Limited, First South Asian Edition, 1998.
- [53] R.G. Parr, W. Yang, Density Functional Theory of Atoms and Molecules, Oxford Science Publication, New York, 1989.
- [54] R.G. Parr, R.G. Pearson, J. Am. Chem. Soc. 105 (1983) 7512.
- [55] P.K. Chattaraj, A. Cedillo, R.G. Parr, E.M. Arnett, J. Org. Chem. 60 (1995) 4707.
- [56] R.G. Parr, Pratim K. Chattaraj, J. Am. Chem. Soc. 113 (1991) 1854.
- [57] C.M. Tice, B. Ganem, J. Org. Chem. 48 (1983) 5048.
- [58] R. Huisgen, G. Molston, E. Langhals, J. Am. Chem. Soc. 108 (1986) 6401.
- [59] R.A. Firestone, Heterocycles 25 (1987) 61.
- [60] W. Benchouk, S.M. Mekelleche, J. Mol. Struct.: THEOCHEM 862 (2008) 1.
- [61] M. Frederickson, Tetrahedron 53 (1997) 403.